J Mater Sci (2015) 50:6388–6394
DOI 10.1007/s10853-015-9191-x

Synthesis of conjugated microporous polymers for gas storage and selective adsorption

Qian Shi[1] · Hanxue Sun[1] · Ruixia Yang[2] · Zhaoqi Zhu[1] · Weidong Liang[1] · Dazhi Tan[3] · Baoping Yang[1] · An Li[1] · Weiqiao Deng[2]

Received: 15 May 2015 / Accepted: 17 June 2015 / Published online: 24 June 2015

Abstract Two novel CMPs networks with ($A_4 + B_3$) type and ($A_4 + B_2$) type were synthesized by Pb(II)/Cu(I)-catalyzed Sonogashira–Hagihara cross-coupling polymerization. The resulting CMPs show high thermal stability with a decomposition temperature above 300 °C. The CMPs exhibit high specific surface areas up to 788 $m^2\ g^{-1}$. Using them as porous platforms, the CO_2 adsorption of CMPs was investigated. Meanwhile, the synthesized CMPs show surface superhydrophobicity with water contact angle about 157° due to the microporous morphological structures and the strongly hydrophobic chemical compositions. The organic liquid uptake of CMPs samples was measured up to 1522 wt% for a variety of organic solvents. Furthermore, simply coating of the resulting CMPs on the stainless steel grid enables the wettability of grid changing from hydrophilicity to superhydrophobicity and superoleophilicity, which makes them potential candidates for selective adsorption of oils and organics from water.

✉ An Li
lian2010@lut.cn

✉ Weiqiao Deng
dengwq@dicp.ac.cn

[1] College of Petrochemical Technology, Lanzhou University of Technology, Langongping Road 287, Lanzhou 730050, People's Republic of China

[2] State Key Laboratory of Molecular Reaction Dynamics, Dalian National Laboratory for Clean Energy, Dalian Institute of Chemical Physics, Chinese Academy of Sciences, Dalian 116023, People's Republic of China

[3] State Key Laboratory of Fine Chemicals, Dalian University of Technology, Dalian 116024, China

Introduction

Microporous framework materials, including zeolites [1], metal–organic frameworks (MOFs) [2, 3], and covalent organic frameworks (COFs) [4, 5], have recently been the subject of intense interest. Taking advantage of the large surface areas, microporosity as well as the large pore volume, these crystalline framework materials are of great importance in many applications such as molecular separations and catalysis [6, 7]. However, the limited physicochemical stability of the most porous examples of the MOFs and COFs is one of big obstacles hindering their practical applications.

As a kind of porous materials, in contrast, microporous organic polymers (MOPs) take great advantages of high design flexibility in functionalization and high stability to air, moistures, and much more rigorous conditions in the most cases [8], though they usually formed in amorphous porous structures. So far, several different classes of organic microporous networks have been synthesized, including covalent triazine-based frameworks (CTFs) [9, 10], hyper-cross-linked polymers [11], polymers of intrinsic microporosity (PIM) [12], and so on. Among these MOPs, conjugated microporous polymers (CMPs) are a new subclass of MOPs and have received much more attentions due to their rigid π-conjugated structure, larger surface areas, high thermal, and chemical stability, which have found a variety of potential applications such as gas storage [13–15], hydrogen production [16, 17], catalysis [18, 19], supercapacitors [20], light harvesting [21], absorption [22], etc. In all of these applications, the porosity of the CMPs is essential as a kind of functional porous medium. At this point, CMPs take great advantage of the designable flexibility of their π-conjugated networks, making it possible to finely tune their porosity by varying the strut length of the monomers, which have been well studied by Cooper et al. [8].

In our previous studies, a variety of CMPs with different morphologies and functionalities have been designed and synthesized as porous mediums for various purposes including hydrogen storage [23, 24], CO_2 capture [25–27], iodine capture [27], composites [28], and oil absorption [22, 29–31]. In particular, we firstly reported the superhydrophobic and superoleophilic wettabilities of the CMPs [22]. Such superwetting property of the CMPs enables the selective absorption of oils and organic solvents from water by simply applying them into oils (organics)/water system, which opens a new way to address the environmental issues especially for the global scale of severe water pollution arising from oil spills and industrial organic pollutants. To achieve better adsorption performance as well as good adsorption selectivity in organics/water systems, it is important to design the new CMPs with suitable porosity and morphology, which are two key factors that should be taken into account since both adsorption performance (porous property) and adsorption selectivity (surface superhydrophobicity and superoleophilicity) are closely relative to these two factors [32–34]. Along this line, several kinds of CMPs were synthesized by us through direct ($A_3 + B_2$) Pd-catalyzed cross-coupling polycondensation in this direction [35, 36]. Therefore, further exploitation of new types monomers and thus preparation of novel CMPs with high performance should be of special interest. In this work, two kinds of CMPs network with ($A_4 + B_3$) type and ($A_4 + B_2$) type were synthesized. Both the samples show superhydrophobic and superoleophilic wettabilities and abundant porosity with a specific surface area up to 788 $m^2\ g^{-1}$, which may found useful applications as porous medium for gas storage and water treatment.

Experimental section

Materials

1,3,5-triethynylbenzene and 1,4-diethynylbenzene were obtained from TCI Co., Ltd. Tetra(4-bromophenyl)methane was purchased from Nanjing Huang Minglong Chemical Technology Co., Ltd. Copper (I) iodide and tetrakis (triphenylphosphine) palladium (0) were obtained from J & K. All chemicals were used as received.

Synthesis

CMPs were synthesized by palladium-catalyzed Sonogashira–Hagihara cross-coupling polymerization [8]. In a typical experimental procedure, 1,3,5-triethynylbenzene and tetra(4-bromophenyl)methane, tetrakis (triphenylphosphine) palladium(0), and copper(I) iodide were dissolved in the mixture of toluene and triethylamine. After stirring for 20 min in N_2 atmosphere, the mixture was heated to 80 °C and kept for 24 h in N_2 atmosphere. After cooling to room temperature, the product was washed by chloroform, acetone, water, and methanol, followed by purification using Soxhlet extraction with methanol for 72 h. Then, the brown-yellow polymer was dried at 70 °C for 24 h and named as BCMP-1. BCMP-2 was synthesized by the same method as mentioned above using 1,4-diethynylbenzene and tetra(4-bromophenyl)methane as monomers.

Characterization

Fourier transform infrared spectroscopy (FTIR) spectra were recorded in the range of 4000–400 cm^{-1} using the KBr pellet technique on an FT-Raman Module instrument (Nicolet FTIR 360). High-resolution imaging of the polymer morphology was achieved using a scanning electron microscopy (SEM, JSM-6701F). The porosity of materials was investigated at 77.3 K using a pore and surface analyzer (Micrometrics, ASAP 2020). Before analysis, the CMPs were degassed at 100 °C for 3 h under vacuum. The thermal properties of the samples were tested by a thermogravimeter (TGA/DSC1, Mettle Toledo), and all of the measurements were carried out under N_2 gas from room temperature to 900 °C with a thermal velocity of 10 °C min^{-1}.

Results and discussion

The BCMP-1 and BCMP-2 were synthesized by Pb(II)/Cu(I)-catalyzed Sonogashira–Hagihara cross-coupling polymerization from tetra(4-bromophenyl)methane and arylethynylene with different structures, which was proved as a reliable approach to construct CMPs networks [8, 27]. The representative molecular structures for BCMP-1 and BCMP-2 are shown in Fig. 1. The molecular level structures of CMPs were investigated by ^{13}C solid-state NMR measurements. Both the BCMP-1 and BCMP-2 exhibited peaks at around 132 and 124 ppm for aromatic peaks, corresponding to C_{Ar}–H and C_{Ar}–C≡C. The peak at 90 ppm was assigned to C_{Ar}–C≡C for quaternary alkynes. A weak peak appeared around 82 ppm could be contributed to the C_{Ar}–C≡C–H for the terminal alkynes. Besides, the peak at ca. 65 ppm was assigned to the central C of the tetraphenylmethane core, indicating that this structure remained intact during the coupling polymerization [37]. FTIR spectra for the BCMP-1 and BCMP-2 are shown in Fig. 2. Both the BCMP-1 and BCMP-2 exhibited similar FTIR spectrum, which suggested the similarity of chemical functional groups.

The FTIR spectra of both the BCMP-1 and BCMP-2 showed four main adsorption regions, as shown in Fig. 3a. The first adsorption bands in the range of 650–1250 cm^{-1}

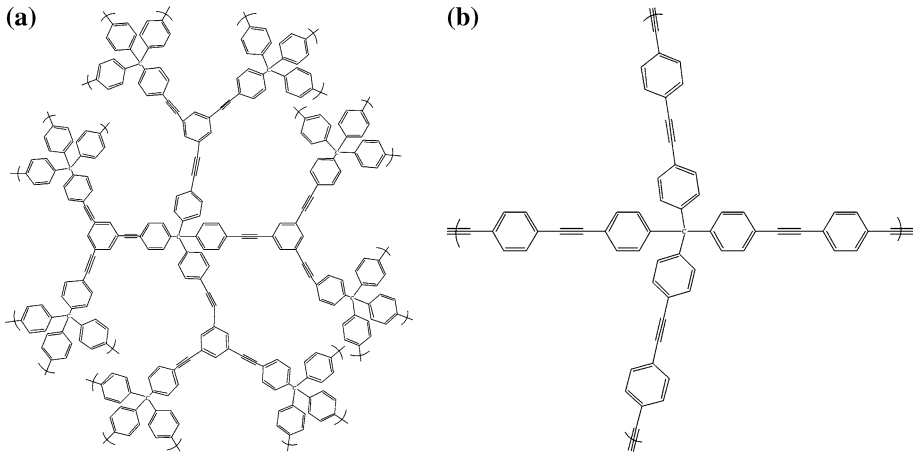

Fig. 1 Schematic representation of **a** BCMP-1 and **b** BCMP-2 networks

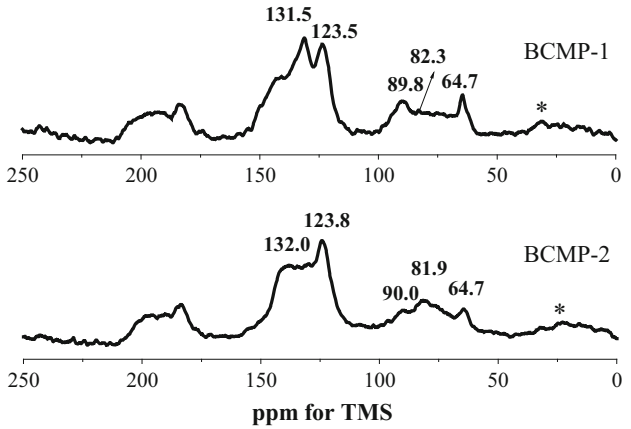

Fig. 2 Solid-state ^{13}C NMR spectra for the BCMP-1 and BCMP-2 networks. *Asterisks* denote spinning sidebands

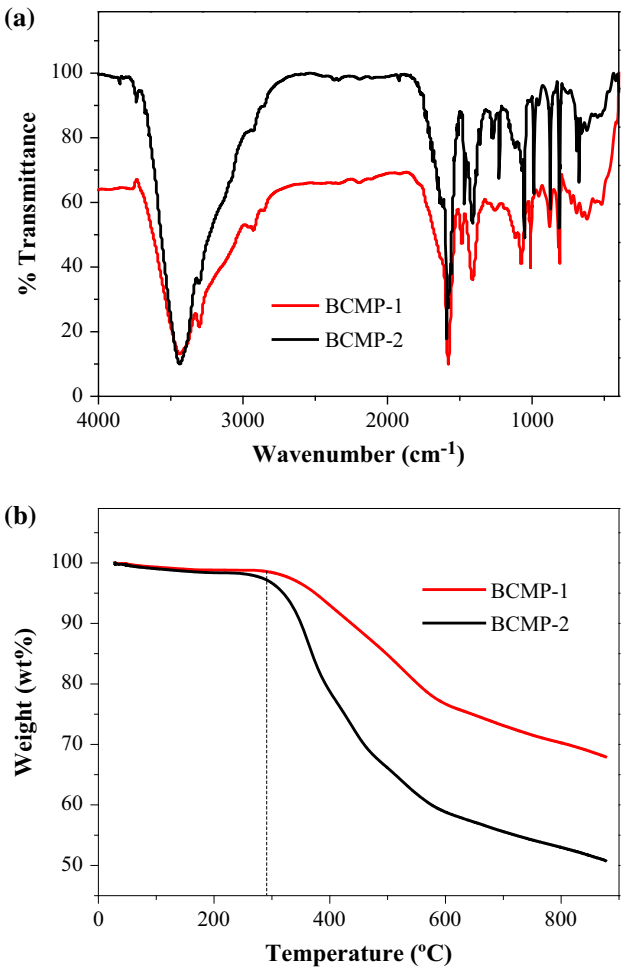

Fig. 3 **a** FTIR spectra of the BCMP-1 and BCMP-2. **b** TGA curves of BCMP-1 and BCMP-2

were assigned to C–H bending vibration of benzene ring. The second adsorption bands at 1400–1650 cm^{-1} corresponded to skeletal vibration of benzene ring. The third peak at 2200–2350 cm^{-1} corresponded to –C≡C– vibration stretching and the fourth peak near 2900 cm^{-1} was assigned to the –Ar–H stretching [28, 30]. FTIR spectra demonstrated that BCMP-1 and BCMP-2 mainly consisted of aromatic rings and C≡C bonds, in accordance with the ^{13}C NMR analysis and Fig. 1. The thermal stability of BCMP-1 and BCMP-2 was investigated by TGA measurement under N_2 atmosphere, as shown in Fig. 3b. No obvious weight loss was observed before 300 °C both for BCMP-1 and BCMP-2, suggesting good thermal stability, which should be contributed to the rigid three-dimensional networks originating from butadiynylene linkages for BCMP-1 and BCMP-2. The weight loss of BCMP-1 was 32 wt%, much lower than that of BCMP-2 above 900 °C, due to its dendritic structure which could be favorable to slow down the heat transmission thus in turn enhancing its thermal stability. The microstructure and morphology of BCMP-1 and BCMP-2 were investigated by SEM. As seen in Fig. 4, both the BCMP-1 and BCMP-2 were composed of agglomerated and nano-sized microgel particles. Furthermore, BCMP-1 and BCMP-2 exhibited amorphous

feature and no evidence of long range molecular order is found, as found in other CMPs materials [8, 22].

The porosity of the samples was evaluated by the N_2 adsorption and desorption isotherms measured at 77.3 K. As shown in Fig. 5a, both BCMP-1 and BCMP-2 exhibited obvious N_2 uptake at low relative pressure (<0.1), indicating microporous features. N_2 uptake continuously increased with the increase of pressure, and a hysteresis loop was observed in the relative pressure range from 0.4 to 0.9, suggesting the existence of a fraction mesoporous pores. At high relative pressure (>0.9), the N_2 adsorption branch exhibited a large increase with typical macroporous feature. The BET surface areas calculated in the relative pressure (P/P_0) between 0.06 and 0.2 from the N_2 adsorption and desorption isotherms were 788 and 490 $m^2\ g^{-1}$. The micropore surface area calculated from *t*-plot method was 294 and 181 $m^2\ g^{-1}$ for BCMP-1 and BCMP-2. Both SCMP-1 and SCMP-2 have relatively narrow pore size distribution (PSD) curves with uppermost peaks at around 2.0 nm, as shown in Fig. 5a inset. The total pore volume was 1.08 and 0.63 $cm^3\ g^{-1}$, and the micropore volume was 0.13 and 0.08 $cm^3\ g^{-1}$ for SCMP-1 and SCMP-2. The micropore ratio was 12.0 and 12.7 wt% for SCMP-1 and SCMP-2.

The control of anthropogenic CO_2 emissions from great consumption of hydrocarbon fuels is a great urgency both for scientific and social community, in view of the significant contribution of CO_2 to the global warming and other climate change issues. To this end, porous organic polymers have been developed and exhibited high CO_2 adsorption capacity [38]. CMPs have also demonstrated great potential in the application for CO_2 capture and storage, due to its abundant porosity, high specific surface areas, and good stability. In this case, the CO_2 uptake capacities of the BCMP-1 and BCMP-2 were investigated at 273 K and 1 bar. As shown in Fig. 5b, the maximum CO_2 uptake of BCMP-1 and BCMP-2 was found to be 66.4 and 67.3 mg g^{-1}. This value is lower than that of functionalized CMPs [25, 39, 40], mainly because of the low

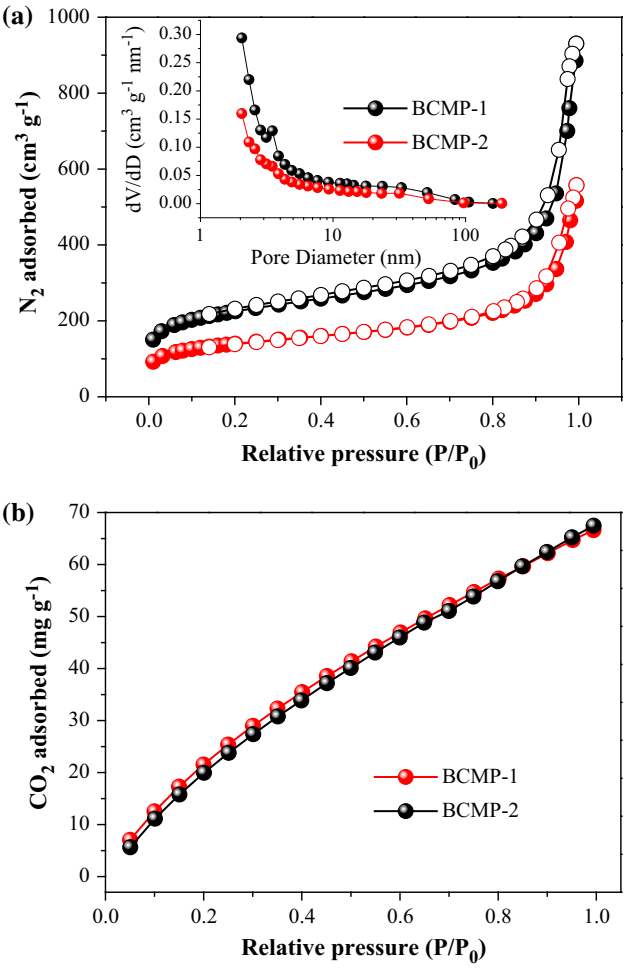

Fig. 5 **a** Nitrogen adsorption (*filled symbols*) and desorption (*open symbols*) isotherms measured at 77 K for BCMP-1 and BCMP-2. *Inset* is the PSD curves for BCMP-1 and BCMP-2. **b** CO_2 adsorption isotherms of BCMP-1 and BCMP-2 at 273 K

micropore volume of samples (0.13 and 0.08 $cm^3\ g^{-1}$ for BCMP-1 and BCMP-2) which is one of the key factors that affect the gas uptake performance of a porous material [24]. However, based on its structure tunability, further

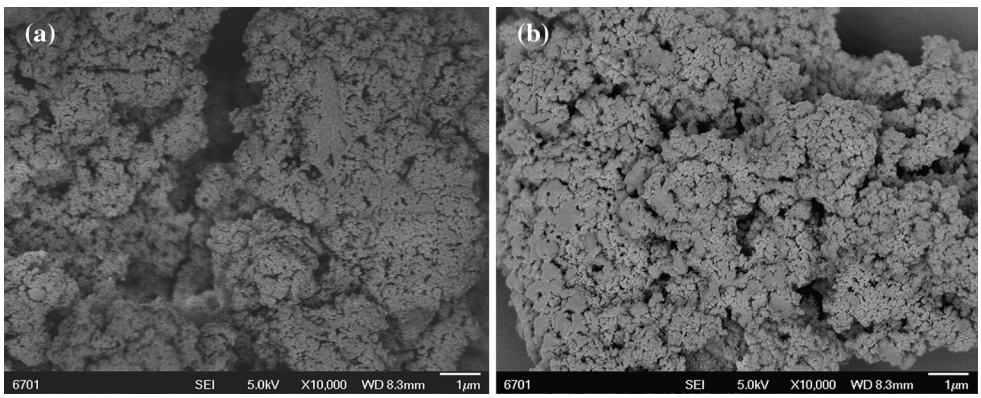

Fig. 4 SEM images of **a** BCMP-1 and **b** BCMP-2. *Scale bar* **a**, **b** 1 μm

enhancement on their CO_2 uptake performance can be anticipated by fine tuning their porosity as well as improving their CO_2 adsorption enthalpies.

Besides, the BCMP-1 and BCMP-2 could absorb organic liquids (especially non-polar or weakly polar organics) and oils from water due to their excellent porosity and surface wettability. To evaluate the surface wettability of BCMP-1 and BCMP-2, static water and oil contact angle (CA) measurements were performed. As shown in Fig. 6a (left), the water CA of BCMP-1 reached up to be 158°, which was called superhydrophobicity [32]. Similar observation was found for the BCMP-2, which also exhibited surface superhydrophobicity with water CA of 157°. On the other hand, the octane CA for BCMP-1 was nearly 0° (Fig. 6a right), suggesting their superoleophilicity. Such excellent surface wettability should be attributed to the microporous morphological structures and the strongly hydrophobic chemical compositions, which totally consists of aromatic rings and –C≡C– bonds [22]. Taking advantages of the excellent surface superhydrophobicity and superoleophilicity, BCMP-1 and BCMP-2 should be candidates for removal of organics from water. The adsorption capacity of CMPs for different organic solvents was investigated by weight gain. The weight gain ratio of the CMPs was defined as ω, which can be calculated as following: $\omega = (M_{absorbed} - M_{dry})/M_{dry} \times 100$ wt%. As shown in Fig. 6b, the BCMP-1 and BCMP-2 show adsorption capacity with 476–1522 and 235–976 wt%. In particular, for those toxic contaminants in water, such as nitrobenzene and trichloromethane, the adsorption capacities of BCMP-1 reach up to 1010 and 1522 wt%. The adsorption capacity of BCMP-1 was greater than that of BCMP-2, due to its higher BET surface area and pore volume, which was favorable to liquid adsorption.

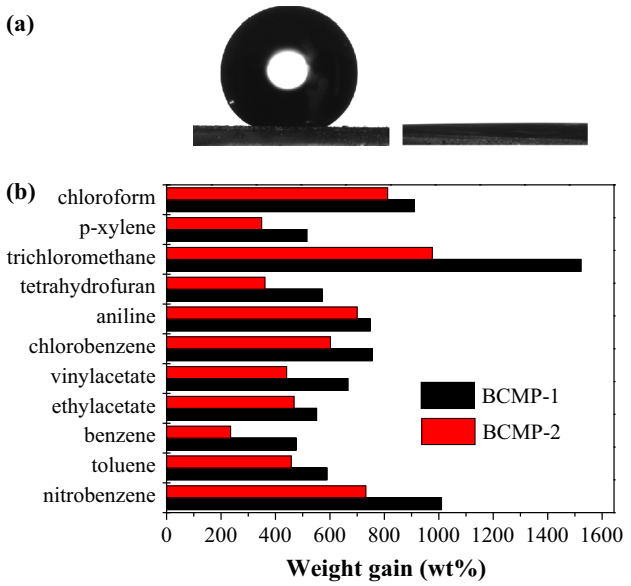

Fig. 6 **a** The water CA (*left*) and octane (*right*) measurement for BCMP-1. **b** The adsorption capacity of BCMP-1 and BCMP-2 for different organic solvents and oils

Most interestingly, we found that the BCMP-1 and BCMP-2 microgel particles could be easily loaded on porous substrates for fabrication of efficient absorbents and filtration materials with high selectivity for organics and water. In this case, BCMP-1 was used as functional coating and its microgel particles could be easily loaded on commercially available stainless steel grids (140 mesh) which were commonly used as filtration film in industry. As expected, simply coating of the resulting CMPs on the stainless steel grid enables the wettability of grid changing from hydrophilicity to superhydrophobicity and superoleophilicity. As shown in Fig. 7a, the water droplets kept spherical on the grid of stainless steel, while the octane quickly spreads and penetrates through the grid pores, due to the excellent surface superhydrophobicity of BCMP-1. Figure 7b exhibits that the BCMP-1 loading stainless steel film could be used for separation of octane (red oil O dyed) and water (methyl blue dyed), showing great potentials in purification, oil spills cleanup, water treatment, and so on. Similar superhydrophobic and superoleophilic mesh films have also been reported by others [41, 42] and us [34] previously. Quite different from those superhydrophobic mesh films constructed by controlling the surface morphological features where surface wettability is greatly

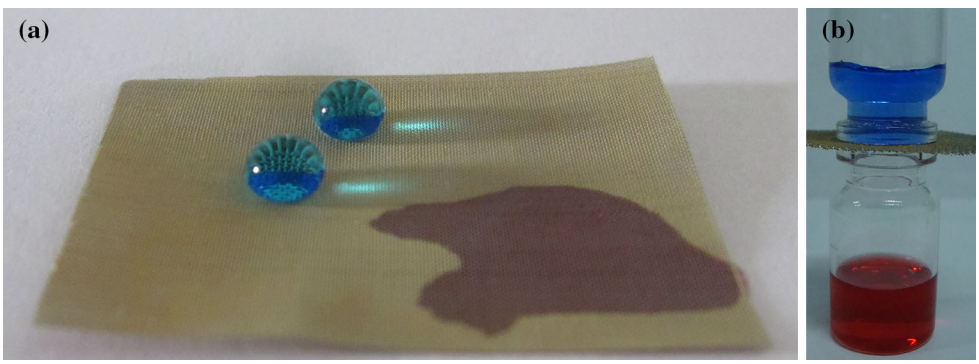

Fig. 7 **a** Water droplets and octane on the surface of BCMP-1 loading stainless steel film. **b** The BCMP-1 loading stainless steel film used for separation of octane (*red oil O dyed*) and water (*methyl blue dyed*) (Color figure online)

influenced by experimental conditions or techniques adopted, our strategy takes advantage of inherent chemistry of BCMP-1 which allows both strong hydrophobic chemical compositions and well-defined microporous characteristics are easily obtained at the same time to create a superhydrophobic surface only through a facile painting process without any complicated techniques.

Conclusion

Two novel CMPs BCMP-1 and BCMP-2 were designed and synthesized by Pb(II)/Cu(I)-catalyzed Sonogashira–Hagihara cross-coupling polymerization. Both BCMP-1 and BCMP-2 exhibited high thermal stability with a decomposition temperature above 300 °C. The BET surface areas of BCMP-1 and BCMP-2 were 788 and 490 $m^2\ g^{-1}$, and the maximum CO_2 uptake could be reached up to 66.4 and 67.3 mg g^{-1} at 273 K and 1 bar. Meanwhile, both BCMP-1 and BCMP-2 exhibited surface superhydrophobicity with water CA of 157° and 158°, which should be contributed to the microporous morphological structures and the strongly hydrophobic chemical compositions of BCMP-1 and BCMP-2. The BCMP-1 and BCMP-2 show adsorption capacity with 476–1522 and 235–976 wt% for a variety of organic solvents. Furthermore, simply coating of the BCMP-1 microgel particles on the stainless steel grid enables the wettability of grid changing from hydrophilicity to superhydrophobicity and superoleophilicity, which makes them potential candidates for selective adsorption of oils and organics from water.

Acknowledgements The authors are grateful to the National Natural Science Foundation of China (Grant No. 51263012, 51262019, 51462021 and 51403092), Gansu Provincial Science Fund for Distinguished Young Scholars (Grant No. 1308RJDA012), Hongliu Elitist Scholars of LUT, Fundamental Research Funds for the Universities of Gansu Province, and State Key Laboratory of Fine Chemicals (KF 1310), Dalian University of Technology.

References

1. Spoto G, Bjørgen M, Lillerud KP (2005) Liquid hydrogen in protonic chabazite. J Am Chem Soc 127:6361–6366
2. Li HL, Eddaoudi M, O'Keeffe M, Yaghi OM (1999) Design, synthesis of an exceptionally stable and highly porous metal-organic framework. Nature 402:276–279
3. Zhao XB, Xiao B, Fletcher AJ, Thomas KM, Bradshaw D, Rosseinsky MJ (2004) Hysteretic adsorption and desorption of hydrogen by nanoporous metal-organic frameworks. Science 306:1012–1015
4. Cote AP, Benin AI, Ockwig NW, O'Keeffe M, Matzger AJ, Yaghi OM (2005) Porous, crystalline, covalent organic frameworks. Science 310:1166–1170
5. El-Kaderi HM, Hunt JR, Mendoza-Cortes JL, Cote AP, Taylor RE, O'Keeffe M, Yaghi OM (2007) Designed synthesis of 3D covalent organic frameworks. Science 316:268–272
6. Kaur P, Hupp J, Nguyen ST (2011) Porous organic polymers in catalysis: opportunities and challenges. ACS Catal 1:819–835
7. Lu W, Yuan D, Zhao D, Schilling CI, Plietzsch O, Muller T, Bräse S, Guenther J, Blümel J, Krishna R, Li Z, Zhou H-C (2010) Porous polymer networks: synthesis, porosity and applications in gas storage/separation. Chem Mater 22:5964–5972
8. Jiang J-X, Su F, Trewin A, Wood CD, Niu H, Jones JTA, Khimyak YZ, Cooper AI (2008) Synthetic Control of the pore dimension and surface area in conjugated microporous polymer and copolymer networks. J Am Chem Soc 130:7710–7720
9. Bojdys MJ, Jeromenok J, Thomas A, Antonietti M (2010) Rational extension of the family of layered, covalent, triazine-based frameworks with regular porosity. Adv Mater 22:2202–2205
10. Kuhn P, Antonietti M, Thomas A (2008) Porous, Covalent triazine-based frameworks prepared by ionothermal synthesis. Angew Chem Int Ed 47:3450–3453
11. Wood CD, Tan B, Trewin A, Su F, Rosseinsky MJ, Bradshaw D, Sun Y, Zhou L, Cooper AI (2008) Microporous organic polymers for methane storage. Adv Mater 20:1916–1921
12. Ghanem BS, Msayib KJ, McKeown NB, Harris KDM, Pan Z, Budd PM, Butler A, Selbie J, Book D, Walton A (2007) Self-association based on orthogonal C=O···C=O interactions in the solid and liquid state. Chem Commun 46:67–69
13. Wood CD, Tan B, Trewin A, Niu HJ, Bradshaw D, Rosseinsky MJ, Khimyak YZ, Campbell NL, Kirk R, Stockel E, Cooper AI (2007) Hydrogen storage in microporous hypercrosslinked organic polymer networks. Chem Mater 19:2034–2048
14. Budd PM, Butler A, Selbie J, Mahmood K, McKeown NB, Ghanem B, Msayi K, Book D, Walton A (2007) The potential of organic polymer-based hydrogen storage materials. Phys Chem Chem Phys 9:1802–1808
15. Dawson R, Adams DJ, Cooper AI (2011) Chemical tuning of CO_2 sorption in robust nanoporous organic polymers. Chem Sci 2:1173–1177
16. Schwab MG, Hamburger M, Feng X, Shu J, Spiess HW, Wang X, Antonietti M, Mullen K (2010) Photocatalytic hydrogen evolution through fully conjugated poly(azomethine) networks. Chem Commun 46:8932–8934
17. Wang X, Maeda K, Thomas A, Takanabe K, Xin G, Carlsson JM, Domen K, Antonietti M (2009) A metal-free polymeric photocatalyst for hydrogen production from water under visible light. Nat Mater 8:76–80
18. Wang X, Maeda K, Chen X, Takanabe K, Domen K, Hou Y, Fu X, Antonietti M (2009) Polymer semiconductors for artificial photosynthesis: hydrogen evolution by mesoporous graphitic carbon nitride with visible light. J Am Chem Soc 131:1680–1681
19. Jiang JX, Wang C, Laybourn A, Hasell T, Clowes R, Khimyak YZ, Xiao J, Higgins SJ, Adams DJ, Cooper AI (2011) Metal-organic conjugated microporous polymers. Angew Chem Int Ed 250:1072–1075
20. Kou Y, Xu Y, Guo Z, Jiang DL (2011) Supercapacitive energy storage and electric power supply using an aza-fused π-conjugated microporous framework. Angew Chem Int Ed 50:8753–8757
21. Chen L, Honsho Y, Seki S, Jiang D (2010) Light-harvesting conjugated microporous polymers: rapid and highly efficient flow of light energy with a porous polyphenylene framework as antenna. J Am Chem Soc 132:6742–6748
22. Li A, Sun HX, Tan DZ, Fan WJ, Wen SH, Qing XJ, Li GX, Li SY, Deng WQ (2011) Superhydrophobic conjugated microporous polymers for separation and adsorption. Energy Environ Sci 4:2062–2065
23. Tan D, Fan W, Xiong W, Sun H, Li A, Deng W, Meng C (2012) Study on adsorption performance of conjugated microporous polymers for hydrogen and organic solvents: the role of pore volume. Eur Polym J 48:705–711
24. Li A, Lu R-F, Wang Y, Wang X, Han K-L, Deng W-Q (2010) Lithium-doped conjugated microporous polymers for reversible hydrogen storage. Angew Chem Int Ed 49:3330–3333

25. Xie Y, Wang TT, Liu XH, Zou K, Liu XH, Deng WQ (2013) Capture and conversion of CO_2 at ambient conditions by a conjugated microporous polymer. Nat Commun 4:1960–1965
26. Xie Y, Wang TT, Yang RX, Huang NY, Zou K, Deng WQ (2014) Efficient fixation of CO_2 by a zinc-coordinated conjugated microporous polymer. ChemSusChem 7:2110–2114
27. Chen Y, Sun H, Yang R, Wang T, Pei C, Xiang Z, Zhu Z, Liang W, Li A, Deng W (2015) Synthesis of conjugated microporous polymer nanotubes with large surface areas as absorbents for iodine and CO_2 uptake. J Mater Chem A 3:87–91
28. Xiang Z, Sun H, Zhu Z, Liang W, Yang B, Li A (2015) Synthesis of conjugated microporous polymer nanotubes for polymer composites. RSC Adv 5:24893–24898
29. Tan D, Fan W, Xiong W, Sun H, Cheng Y, Liu X, Meng C, Li A, Deng WQ (2012) Study on the morphologies of covalent organic microporous polymers: the role of reaction solvents. Macromol Chem Phys 213:1435–1440
30. Tan D, Xiong W, Sun H, Zhang Z, Ma W, Meng C, Fan W, Li A (2013) Conjugated microporous polymer with film and nanotube-like morphologies. Microporous Mesoporous Mater 176:25–30
31. Fan W, Liu X, Zhang Z, Zhang Q, Ma W, Tan D, Li A (2014) Conjugated microporous polymer nanotubes and hydrophobic sponges. Microporous Mesoporous Mater 196:335–340
32. Feng L, Li S, Li Y, Li H, Zhang L, Zhai J, Song Y, Liu B, Jiang L, Zhu D (2002) Super-hydrophobic surfaces: from natural to artificial. Adv Mater 14:1857–1860
33. Sun H, Li A, Zhu Z, Liang W, Zhao X, La P, Deng W (2013) Superhydrophobic activated carbon-coated sponges for separation and absorption. ChemSusChem 6:1057–1062
34. Sun H, Li A, Qin X, Zhu Z, Liang W, An J, La P, Deng W (2013) Three-dimensional superwetting mesh film based on graphene assembly for liquid transportation and selective absorption. ChemSusChem 6:2377–2381
35. Dawson R, Laybourn A, Clowes R, Khimyak YZ, Adams DJ, Cooper AI (2009) Functionalized conjugated microporous polymers. Macromolecules 42:8809–8816
36. Dawson R, Laybourn A, Khimyak YZ, Adams DJ, Cooper AI (2010) High surface area conjugated microporous polymers: the importance of reaction solvent choice. Macromolecules 43:8524–8530
37. Choi JH, Choi KM, Jeon HJ, Choi YJ, Lee Y, Kang JK (2010) Acetylene gas mediated conjugated microporous polymers (ACMPs): first use of acetylene gas as a building unit. Macromolecules 43:5508–5511
38. McKeown NB, Budd P (2006) Polymers of intrinsic microporosity (PIMs): organic materials for membrane separations, heterogeneous catalysis and hydrogen storage. Chem Soc Rev 35:675–683
39. Qiao S, Du Z, Yang C, Zhou Y, Zhu D, Wang J, Chen X, Yang R (2014) Phosphine-containing microporous networks: high selectivity toward carbon dioxide to methane. Polymer 55:1177–1182
40. Dawson R, Stöckel E, Holst JR, Adams DJ, Cooper AI (2011) Microporous organic polymers for carbon dioxide capture. Environ Sci 4:4239–4245
41. Feng L, Zhang Z, Mai Z, Ma Y, Liu B, Jiang L, Zhu D (2004) A super-hydrophobic and super-oleophilic coating mesh film for the separation of oil and water. Angew Chem Int Ed 43:2012–2014
42. Wang CF, Tzeng FS, Chen HG, Chang CJ (2012) Ultraviolet-durable superhydrophobic zinc oxide-coated mesh films for surface and underwater-oil capture and transportation. Langmuir 28:10015–10019